assessments. To minimize a possible detection of RNA species degraded from dying cells at this toxicity level, the culture dishes were thoroughly washed three times by PBS before harvesting to remove the dead cells and degraded molecules. For the gene expression microarray experiment, 40 mg/ml of silver-NP-hydrogel was used. The cells were seeded at a concentration of 5×10^5 cells/35-cm cell culture dish for CBMN assay, MTT assay and DNA microarray experiment. The cells were exposed to the silver-NP-hydrogel for 24 and 48 h, respectively.

CBMN assay

The CBMN assay was carried out using the protocol described as below. Briefly, the HeLa cells were seeded and maintained to 70–80% confluence at 24 h. Silver-NP-hydrogel was added to culture media at concentrations of 20, 40 and 60 mg/ml respectively, and after ultrasonic treatment (300 W, 42 kHz for 10 min) the media with silver-NP-hydrogel was applied to the cells. MMC (0.1 μg/ml) was used as a positive control, and NaCl (50 μl/ml) was used as a negative control. The cells were then further cultured for 24 h. After washing thoroughly with three times of PBS, Cytochalasin-B (final conc., 3 μg/ml) was added to the cells, and the cells were cultured for another 18 h. The cells were subsequently collected. After a hypotonic treatment in 2 ml of 0.075 M KCl at room temperature for 5 min, the cells were fixed using methyl alcohol:acetic acid (3:1). The cells were then placed onto a slide, dried at room temperature, and stained using 4% Giemsa solution (pH 6.8) for 30 min.

The slides were scored at 400× magnification blindly by two investigators separately. The micronucleation frequency (MNF, %) was determined for 1000 binucleated cells (BNCs).

Total RNA isolation and DNA microarray

The cells reached 70–85% confluence at both 24 h and 48 h cultures with the treatment of silver-NP-hydrogel at a concentration of 40 mg/ml, and almost a full conference in the control cultures with non-treatment (Figure 2). The total RNA from each sample was extracted from the HeLa cells using ISOGEN RNA isolation reagent (Nippon gene, Japan) according to the instructions provided by the manufacturer. After decontamination treatment of genomic DNA using DNase I digestion, the quality and integrity of the RNA samples were determined by appearance of the distinct 28 S and 18 S bands of ribosomal RNA on agarose gel electrophoresis. Total RNA purity was measured spectrophotometrically by the absorbance ratio 260/280 nm. Results ranged between 1.7–2.1.

A gene expression study was conducted using "Two-color microarray-based gene expression analysis" (Agilent technologies, USA, Whole Human Genome Microarray 4x44K, G4110F containing 41000 of DNA oligomer unique probes). Briefly, 1 μg of each sample of RNA was amplified using an Amino Allyl MessageAmp II aRNA Amplification Kit (Ambion, USA). Amplified RNA (aRNA) was labeled using Cy5 and Cy3 according to the instructions provided by the manufacturer. The silver-NP-hydrogel or hydrogel-alone exposure samples were labeled with Cy5, and untreated cells were labeled with Cy3 which was used as control against the treated Cy5-labeled sample. After hybridizing the samples for 16 h at 65°C, the gene chips were washed. The hybridized chips were fluorescently scanned with a microarray scanner (GenePix 4000B, USA) to collect the images. The ratios of intensity ($Log_2Cy5/Cy3$) were calculated and normalized with GenePixPro 6.1 software. Filtering of the results was done as follows: genes were considered as up-regulated when the $Log_2Cy5/Cy3$ ratio was higher than 1 (Cy5/Cy3 was higher than 2) and as down-regulated when the $Log_2Cy5/Cy3$ ratio was lower than −1 (Cy5/Cy3 was lower than −2). Genes were considered as unregulated when the $Log_2Cy5/Cy3$ ratio was between 1 and −1. The GO pathway data was further classified into functional categories. The genes, which were consistently up-regulated and down-regulated at 48 h of silver-NP-hydrogel exposure, were tabled for further analysis.

Gene ontology analysis of gene expression

To determine biological relevant gene ontology terms (GO, provided by NCBI) of differentially expressed genes in HeLa cells, the software "PANTHER", was used. It provides gene expression data analysis/Comparison of gene lists (http://www.pantherdb.org/tools/genexAnalysis.jsp). The analysis was performed using Unigene ID as the identifier for biological process categories.

Real-time PCR

The reliability of the gene expression profile was validated by real-time PCR (SYBR Green method) for five selected genes, viz., interleukin 1, alpha (IL1A); heme oxygenase (decycling) 1(HMOX1); DNA-damage-inducible transcript 3 (DDIT3); metallothionein 1 F (MT1F) and platelet-derived growth factor receptor, beta polypeptide (PDGFRB)

Table 5 Primers used in real-time PCR

Gene	GeneBank	Primer Sequence 5'→3'
Actin	NM 001101	Forward Primer: CATGTACGTTGCTATCCAGGC Reverse Primer: CTCCTTAATGTCACGCACGAT
MT1F	NM 005949	Forward Primer: CCCACTGCTTCTTCGCTTCT Reverse Primer: GAGAAAGGTTGTCCTGGCATC
IL1A	NM 000575	Forward Primer: AATGACGCCCTCAATCAAAGTA Reverse Primer: CTCCTTCAGCAGCACTGGTTG
HMOX 1	NM002133	Forward Primer: AAGAGGCCAAGACTGCGTTC Reverse Primer: GAGTGTAAGGACCCATCGGAGA
DDIT 3	NM 004083	Forward Primer: GTCCTGTCTTGATGAAAATGG Reverse Primer: GTGCTTGTGACCTCTGCTGG
PDGFRB	NM 002609	Forward Primer: GAGACTGTTGGGCGAAGGTTA Reverse Primer: GAGATGGTTGAGGAGGTGTTGAC

at 48 h exposure of silver-NP-hydrogel. Real-time PCR was performed using the ABI 7900 HT Fast RealTime PCR system (Applied Biosystem, USA). Briefly, total RNA (25 μg) from each sample was DNase I digested by the following reactions: RQ1 RNase-Free DNase 10× Reaction Buffer (5 μl), RQ1 RNase-Free DNase I (2 μl,Promega, USA), Recombinant RNasin RNase Inhibitor (1 μl, Promega, USA), Nuclease-Free Water to total volume 50 μl, with incubation for 30 min at 37°C. Following purification of DNase I digested RNA, 2 μg of RNA was reverse-transcribed into cDNA by using M-MLV reverse transcriptase (Invitrogen, USA). One μl of the cDNA sample was added to the PCR mixture which was composed of 10 μl of Power SYBR Green PCR Master Mix (Applied Biosystem, USA), 0.5 μl of forward primer (10 μM) and 0.5 μl of reverse primer (10 μM). Nuclease-free water was added to bring the volume up to 20 μl, and the mixture was subjected to PCR amplification. The primers used in this study are listed in Table 5. The threshold cycles (Ct) in each sample were measured by comparing their amplification with that of standard samples and was normalized to that of the housekeeping gene actin. An average Ct of triplicate detection for each gene, ΔCt (Detecting gene - House keeping gene); and ΔΔCt (Test sample-Control sample) was obtained; finally calculated $2^{-\Delta\Delta Ct}$ and represented as the differential expression of test genes.

Statistical analysis

The data were represented as the mean ± SD. The CBMN assay was repeated three independent times. The data was statistically analyzed using the SPSS, version 12.0.1), the *t*-test, ANOVA and Dunnett test (2-sided). Differences were considered significant if the *P*-value was less than 0.05.

Additional files

Additional file 1: Up-regulated genes in cells exposed to silver-NP-hydrogel for 24 h. Fold-change is logarithmic ratio (log2 ratio) to expression level in control.

Additional file 2: Down-regulated genes in cells exposed to silver-NP-hydrogel for 24 h. Fold-change is logarithmic ratio (log2 ratio) to expression level in control.

Additional file 3: Up-regulated genes in cells exposed to silver-NPs-hydrogel for 48h. Fold-change is logarithmic ratio (log2 ratio) to expression level in control.

Additional file 4: Down-regulated genes in cells exposed to silver-NPs-hydrogel for 48h. Fold-change is logarithmic ratio (log2 ratio) to expression level in control.

Additional file 5: Up-regulated genes in cells exposed to Hydrogel for 24 h. Fold-change is logarithmic ratio (log2 ratio) to expression level in control.

Additional file 6: Down-regulated genes in cells exposed to Hydrogel for 24 h. Fold-change is logarithmic ratio (log2 ratio) to expression level in control.

Additional file 7: Up-regulated genes in cells exposed to Hydrogel for 48h. Fold-change is logarithmic ratio (log2 ratio) to expression level in control.

Additional file 8: Down-regulated genes in cells exposed to Hydrogel for 48 h. Fold-change is logarithmic ratio (log2 ratio) to expression level in control.

Additional file 9: Common up-regulated genes in cells exposed to silver-NP-hydrogel for 24 h and 48 h. Fold-change is logarithmic ratio (log2 ratio) to expression level in control.

Additional file 10: Common down-regulated genes in cells exposed to silver-NP-hydrogel for 24h and 48 h. Fold-change is logarithmic ratio (log2 ratio) to expression level in control.

Additional file 11: Common up-regulated genes in cells exposed to hydrogel for 24 h and 48 h. Fold-change is logarithmic ratio (log2 ratio) to expression level in control.

Additional file 12: Common down-regulated genes in cells exposed to hydrogel for 24 h and 48 h. Fold-change is logarithmic ratio (log2 ratio) to expression level in control.

Additional file 13: Common up-regulated genes in cells exposed to hydrogel and silver-NP-hydrogel for 48h. Fold-change is logarithmic ratio (log2 ratio) to expression level in control.

Additional file 14: Common down-regulated genes in cells exposed to hydrogel and silver-NP-hydrogel for 48h. Fold-change is logarithmic ratio (log2 ratio) to expression level in control.

Additional file 15: Down-regulated genes related to mitosis pathway at silver-NP-hydrogel treatment for 48h.

Additional file 16: Figure S1. The size and size distribution of the silver nanoparticles determined by transmission electron microscopy (TEM). A: X 10000, bar = 200 nm; B: X 20000, bar = 100 nm.

Abbreviations

silver-NP: Silver nanoparticle; silver-NP-hydrogel: Silver nanoparticle based hydrogel; CBMN: Cytokinesis-block micronucleus; ROS: Reactive oxygen species; Cyto-B: Cytochalasin B; DMSO: Dimethyl sulfoxide; MMC: Mitomycin C; MTT: Methyl tetrazolium; GO: Gene ontology; MNF: Micronucleation frequency; BNCs: Binucleated cells; TEA: Triethanolamine; CDC14A: Cell division cycle 14 homolog A; JAK-STAT: Janus kinase/signal transducers and activators of transcription; IFI: Interferon-induced proteins; IFIT: Interferon-induced protein in the tetratricopeptide; IL: Interleukin; IL1A: Interleukin 1 alpha; HMOX1: Heme oxygenase (decycling); DDIT3: DNA-damage-inducible transcript 3; MT1F: Metallothionein 1 F; PDGFRB: Platelet-derived growth factor receptor beta polypeptide.

Competing interests

The authors declare that they have no competing interests.

Acknowledgements

This study was financially supported by the Human Resources and Social Security Office of China (HRSSO Letter [2009], No. 416), the Beijing Natural Science Foundation of China (No. 3112024) and the Open Research Fund of State Key Laboratory of Bioelectronics, Southeast University, China; National Key Technology Research and Development Program of the Ministry of Science and Technology of China (2012BAI22B01, 2012BAK26B00).

Author details

[1]Institute for Medical Devices Control, National Institutes for Food and Drug Control (NIFDC), No. 2 Temple of Heaven, Beijing 100050, China. [2]Baotou Medical College, Inner Mongolia University of Science & Technology, Baotou 014010, China. [3]Interdisciplinary Laboratory for Nanoscale Science and Technology, National Institute for Materials Science, 1-2-1 Sengen, Tsukuba, Ibaraki 305-0047, Japan. [4]Goldman School of Dental Medicine, Boston University, 801 Albany Street, Suite 200, Boston, MA 02118-2392, USA.

Authors' contributions

Liming Xu participated in the design of study, sequence alignment, performed the statistical analysis and drafted the manuscript. Xuefei Li carried out the genotoxic assay, participated in the sequence alignment and drafted the manuscript. Taro Takemura and Nobutaka Hanagata carried out

the DNA microarray experiment and data analysis. Gang Wu and Laisheng Lee Chou participated in the design of study, data analysis and coordination, and drafting manuscript. All authors read and approved the final manuscript.

Received: 7 December 2011 Accepted: 1 May 2012
Published: 1 May 2012

References

1. Lee JH, Chae JD, Kim DG, Hong SH, Lee WM, Ki M: **Comparison of the efficacies of silver-containing dressing materials for treating a full-thickness rodent wound infected by methicillin-resistant Staphylococcus aureus.** *Korean J Lab Med* 2010, **30**:20–27.
2. Elliott C: **The effects of silver dressings on chronic and burns wound healing.** *Br J Nurs* 2010, **19**:532–536.
3. Gabriel MM, Mayo MS, May LL, Simmons RB, Ahearn DG: **In vitro evaluation of the efficacy of a silver-coated catheter.** *Curr Microbiol* 1996, **33**:1–5.
4. Ahearn DG, Grace DT, Jennings MJ, Borazjani RN, Boles KJ, Rose LJ, Simmons RB, Ahanotu EN: **Effects of hydrogel/silver coatings on in vitro adhesion to catheters of bacteria associated with urinary tract infections.** *Curr Microbiol* 2000, **41**:120–125.
5. Wu J, Hou S, Ren D, Mather PT: **Antimicrobial properties of nanostructured hydrogel webs containing silver.** *Biomacromolecules* 2009, **10**:2686–2693.
6. Gils PS, Ray D, Sahoo PK: **Designing of silver nanoparticles in gum arabic based semi-IPN hydrogel.** *Int J Biol Macromol* 2010, **46**:237–244.
7. Thomas V, Yallapu MM, Sreedhar B, Bajpai SK: **A versatile strategy to fabricate hydrogel-silver nanocomposites and investigation of their antimicrobial activity.** *J Colloid Interface Sci* 2007, **315**:389–395.
8. Ji JU, Jung JH, Kim SS, Yoon JU, Park JD, Choi BS, Chung YH, Kwon IU, Jeong J, Han BS, Shin JH, Sung JH, Song KS, Yu IJ: **Twenty-eight-day inhalation toxicity study of silver nanoparticles in Sprague–Dawley rats.** *Inhal Toxicol* 2007, **19**:857–871.
9. Sung JH, Ji JH, Yoon JU, Kim DS, Kim DS, Song MY, Jeong J, Han BS, Han JH, Chung YH, Kim J, Kim TS, Chang HK, Lee EJ, Lee JH, Yu IJ: **Lung function changes in Sprague–Dawley rats after prolonged inhalation exposure to silver nanoparticles.** *Inhal Toxicol* 2008, **20**:567–574.
10. Sung JH, Ji JH, Park JD, Yoon JU, Kim DS, Jeon KS, Song MY, Jeong J, Han BS, Han JH, Chung YH, Chang HK, Lee JH, Cho MH, Kelman BJ, Yu IJ: **Subchronic inhalation toxicity of silver nanoparticles.** *Toxicol Sci* 2009, **108**:452–461.
11. Kim YS, Kim JS, Cho HS, Rha DS, Kim JM, Park JD, Choi BS, Lim R, Chang HK, Chung YH, Kwon IH, Jeong J, Han BS, Yu IJ: **Twenty-eight-day oral toxicity, genotoxicity, and gender-related tissue distribution of silver nanoparticles in Sprague–Dawley rats.** *Inhal Toxicol* 2008, **20**:575–583.
12. Kim YS, Song MY, Park JD, Song KS, Ryu HR, Chung YH, Chang HK, Lee JH, Oh KH, Kelman BJ, Hwang IK, Yu IJ: **Subchronic Oral toxicity of silver nanoparticles.** *Part Fibre Toxicol* 2010, **7**:20.
13. Tang J, Xiong L, Wang S, Wang J, Liu L, Li J, Yuan F, Xi T: **Distribution, translocation and accumulation of silver nanoparticles in rats.** *J Nanosci Nanotechnol* 2009, **9**:4924–4932.
14. Tang J, Xiong L, Zhou G, Wang S, Wang J, Liu L, Jiage Li, Yuan F, Lu S, Wan Z, Chou L, Xi T: **Silver nanoparticles crossing through and distribution in the blood–brain barrier in vitro.** *J Nanosci Nanotechnol* 2010, **10**:6313–6317.
15. Braydich-Stolle L, Hussain S, Schlager JJ, Hofmann MC: **In vitro cytotoxicity of nanoparticles in mammalian germline stem cells.** *Toxicol Sci* 2005, **88**:412–419.
16. Crewlich C, Kittler S, Epple M, Muhr G, Koller M: **Studies on the biocompatibility and the interaction of silver nanoparticles with human mesenchymal stem cells (hMSCs).** *Langenbecks Arch Surg* 2009, **394**:495–502.
17. Hackenberg S, Scherzed A, Kessler M, Hummel S, Technau A, Froelich K, Ginzkey C, Koehler C, Hagen R, Kleinsasser N: **Silver nanoparticles: evaluation of DNA damage, toxicity and functional impairment in human mesenchymal stem cells.** *Toxicol Lett* 2010, **201**:27–33.
18. Greulich C, Diendorf J, Simon T, Eggeler G, Epple M, Köller M: **Uptake and intracellular distribution of silver nanoparticles in human mesenchymal stem cells.** *Acta Biomater* 2011, **7**:347–354.
19. Hussain SM, Hess KL, Gearhart JM, Geiss KT, Schlager JJ: **In vitro toxicity of nanoparticles in BRL 3A rat liver cells.** *Toxicol In Vitro* 2005, **19**:975–983.
20. Hsin YH, Chen CF, Huang S, Shih TS, Lai PS, Chueh PJ: **The apoptotic effect of nanosilver is mediated by a ROS- and JNK-dependent mechanism involving the mitochondrial pathway in NIH3T3 cells.** *Toxicol Lett* 2008, **179**:130–139.
21. Kawata K, Osawa M, Okabe S: **In vitro Toxicity of silver nanoparticles at nanocytotoxic doses to HepG2 human hepatoma cells.** *Environ Sci Technol* 2009, **43**:6046–6051.
22. AshaRani PV, Hande PM, Valiyaveettil S: **Anti-proliferative activity of silver nanoparticles.** *BMC Cell Biology* 2009, **10**:65–79.
23. AshaRani PV, Low Kah MG, Hande MP, Valiyaveettil S: **Cytotoxicity and genotoxicity of silver nanoparticles in human cells.** *ACS nano* 2009, **3**:279–290.
24. Kim HR, Kim MJ, Lee SY, Oh SM, Chung KH: **Genotoxic effects of silver nanoparticles stimulated by oxidative stress in human normal bronchial epithelial (BEAS-2B) cells.** *Mutat Res* 2011, **726**:129–135.
25. Xu L, Takemura T, Xu M, Hanagata N: **Toxicity of silver nanoparticles as assessed by global gene expression analysis.** *Materials Express* 2011, **1**:74–79.
26. Kumari M, Mukherjee A, Chandrasekaran N: **Genotoxicity of silver nanoparticles in Allium cepa.** *Sci Total Environ* 2009, **407**:5243–5246.
27. Boonstra J, Post JA: **Molecular events associated with reactive oxygen species and cell cycle progression in mammalian cells.** *Gene* 2004, **337**:1–13.
28. Xia T, Kovochich M, Brant J, Hotze M, Sempf J, Oberley T, Sioutas C, Yeh JI, Wiesner MR, Nel AE: **Comparison of the abilities of ambient and manufactured nanoparticles to induce cellular toxicity according to an oxidative stress paradigm.** *Nano Lett* 2006, **6**:1794–1807.
29. Carlson C, Hussain SM, Schrand AM, Braydich-Stolle LK, Hess KL, Jones RL, Schlager JJ: **Unique cellular interaction of silver nanoparticles: size-dependent generation of reactive oxygen species.** *J Phys Chem* 2008, **112**:13608–13619.
30. Fenech M: **The advantages and disadvantages of the cytokinesis-block micronucleus method.** *Mutat Res* 1997, **392**:11–18.
31. Chou L: **Molecular biocompatibility.** *J Dent Res* 1995, **74**:190–193.
32. Lu X, Bao X, Huang Y, Qu Y, Lu H, Lu Z: **Mechanisms of cytotoxicity of nickel ions based on gene expression profiles.** *Biomaterials* 2009, **30**:141–148.
33. Lu X, Lu H, Zhao L, Yang Y, Lu Z: **Genome-wide pathways analysis of nickel ion-induced differential genes expression in fibroblasts.** *Biomaterials* 2010, **31**:1965–1973.
34. Kim JS, Sung JH, Ji JH, Song KS, Lee JH, Kang CS, Yu IJ: **In vivo genotoxicity of silver nanoparticles after 90-day silver nanoparticle inhalation exposure.** *Saf Health Work* 2011, **2**:34–38.
35. Xu L, Chen L, Dong Z, Wang J, Wang Z, Shao A: **In vivo toxicity in reproductive organs of rabbit and in vitro cytotoxicity of silver nanoparticle based-hydrogel.** *Chi J Pharm Anal* 2012, **2**:194–201.
36. Becker H, Herzberg F, Schulte A, Kolossa-Gehring M: **The carcinogenic potential of nanomaterials, their release from products and options for regulating them.** *Int J Hyg Environ Health* 2011, **214**:231–238.
37. Sanchez VC, Pietruska JR, Miselis NR, Hurt RH, Kane AB: **Biopersistence and potential adverse health impacts of fibrous nanomaterials: what have we learned from asbestos?** *Wiley Interdiscip Rev Nanomed Nanobiotechnol* 2009, **1**:511–529.
38. Tsui MT, Wang WX: **Biokinetics and tolerance development of toxic metals in Daphnia magna.** *Environ Toxicol Chem* 2007, **26**:1023–1032.
39. Min KS: **Physiological significance of metallothionein in oxidative stress.** *Yakugaku Zasshi* 2007, **127**:695–702.
40. Woo S, Yum S, Jung JH, Shim WJ, Lee CH, Lee TK: **Heavy metal-induced differential gene expression of metallothionein in Javanese medaka, Oryzial javanicus.** *Mar Biotechnol (NY)* 2006, **8**:654–662.
41. Clark JE, Foresti R, Green CJ, Motterlini R: **Dynamics of haem oxygenase-1 expression and bilirubin production in cellular protection against oxidative stress.** *Biochem J* 2000, **384**:615–619.
42. Elbirt KK, Bonkovsky HL: **Heme oxygenase: recent advances in understanding its regulation and role.** *Proc Assoc Am Physicians* 1999, **111**:438–447.
43. Rahman MF, Wang J, Patterson TA, Saini UT, Robinson BL, Newport GD, Murdock RC, Schlager JJ, Hussain SM, Ali SF: **Expression of genes related to oxidative stress in the mouse brain after exposure to silver-25 nanoparticles.** *Toxicol Lett* 2009, **187**:15–21.
44. Wong AK, Chen Y, Lian L, Ha PC, Petersen K, Laity K, Carillo A, Emerson M, Heichman K, Gupte J, Tavtigian SV, Teng DH: **Genomic structure, chromosomal location, and mutation analysis of the human CDC14A gene.** *Genomics* 1999, **59**:248–251.

45. Aaronson DS, Horvath CM: **Road Map for Those Who Don't Know JAK-STAT.** *Science* 2002, **296**:1653–1655.
46. O'Shea JJ, Gadina M, Schreiber RD: **Cytokine Signaling: new Surprises in the Jak/Stat Pathway.** *Cell* 2002, **109**:S121–S131.
47. Imada K, Leonard WJ: **The Jak-STAT pathway.** *Mol Immunol* 2000, **37**:1–11.
48. Hebenstreit D, Horejs-Hoeck J, Duschl A: **JAK/STAT-dependent gene regulation by cytokines.** *Drug News Perspect* 2005, **18**:243–249.
49. Espert L, Dusanter-Fourt I, Chelbi-Alix MK: **Negative regulation of the JAK/STAT: pathway implication in tumorigenesis.** *Bull Cancer* 2005, **92**:845–857.
50. Rakesh K, Agrawal DK: **Controlling cytokine signaling by constitutive inhibitors.** *Biochem Pharmacol* 2005, **70**:649–657.

doi:10.1186/1477-3155-10-16
Cite this article as: Xu *et al.*: Genotoxicity and molecular response of silver nanoparticle (NP)-based hydrogel. *Journal of Nanobiotechnology* 2012 **10**:16.

ORIGINAL ARTICLE

Synergic Toxicity of Solid Particles and Released Zinc from Zinc Oxide Nanoparticles to Human Lung Epithelial Cells

Fei Zhuang[1], and Nobutaka Hanagata[1, 2]

[1]*Graduate School of Life Science, Hokkaido University, Sapporo, Japan.*
[2]*Nanotechnology Innovation Station, National Institute for Materials Science, Tsukuba, Japan.*

Synopsis

To identify the respective contributions of released zinc and solid particles on the cytotoxicity of zinc oxide nanoparticles (ZnO-NPs), we exposed A549 cells to ZnO-NP suspensions, their extractions collected after centrifugation, and medium containing zinc chloride ($ZnCl_2$). We then assayed the cytotoxicity of these samples using water-soluble tetrazolium salts (WSTs) and intracellular reactive oxygen species (ROS) with 2',7'-dichlorodihydrofluorescin diacetate (DCFH-DA) as outputs. Only the ZnO-NP suspension caused cytotoxicity and increased intracellular ROS; the extractions and $ZnCl_2$ did not cause cytotoxicity or oxidative stress. Global gene expression analysis revealed that both $ZnCl_2$-containing medium and the ZnO-NP suspension caused upregulation of the "cadmium binding" gene functional category. This category consisted of metallothioneins (MTs), important zinc-homeostasis proteins. To further investigate the role of MTs in ZnO-NP-dependent cytotoxicity, we inhibited the overexpression of MTs with corresponding siRNA and found that released zinc contributed to ZnO-NP-dependent cytotoxicity. We conclude that both solid particles and released zinc contributed to ZnO-NP-dependent cytotoxicity. Additionally, we propose a synergic relationship between ZnO-NPs and MTs.

Key words: *zinc oxide nanoparticles, synergic cytotoxicity, released zinc, metallothioneins, intracellular reactive oxygen species*

Introduction

Zinc oxide nanoparticles (ZnO-NPs) have been extensively applied in electronics, optoelectronics, gas sensors, sunscreens, and antibacterial coatings due to their unique properties arising from quantum confinement, including antibacterial, antifungal, and ultraviolet filtering properties, as well as high catalytic and photochemical activity [1-4]. However, epidemiological and *in vivo* studies have lagged behind the speed of mass ZnO-NP production, thereby escalating human exposure risks [5, 6]. Unfortunately, reports of ZnO-NP toxicity are becoming more and more common, including reports of toxicity in aquatic organisms, terrestrial animals and plants, and microorganisms [7-10]. *In vitro* studies have also revealed that ZnO-NPs are toxic to various human cell lines, such as lung epithelial cells, aortic endothelial cells, epidermal cells, bronchial epithelial cells, lymphoblastoid cells, lung mesothelioma cells, and fibroblasts [11-18].

Currently, concerns have focused on whether the solid particles or the released zinc is the real toxicant in ZnO-NP-dependent cytotoxicity. On one hand, some findings have indicated

that solid particles play an important role. Moos *et al.* found that contact of particles with the cells was required for ZnO-NP-dependent cytotoxicity [14], while Gojova *et al.* concluded that the internalization of nanoparticles by the cells was necessary for ZnO-NP-induced cytotoxicity [13, 14]. Furthermore, ZnO-NP-dependent cytotoxicity was reported to result from increased intracellular reactive oxygen species (ROS) caused by the solid particles via a special interface chemical activity [12, 17, 19]. In contrast, Franklin *et al.* demonstrated the importance of the solubility of ZnO-NPs for toxicity in microalga [20]. Brunner also found that the solubility of ZnO-NPs was very important for cytotoxicity [18]. Additionally, another study suggested that the particles were internalized by the cells and intracellular released zinc was the true toxicant in ZnO-NP-induced cytotoxicity [21]. Xia and colleagues found accumulation of fluorescein isothiocyanate (FITC)-labeled ZnO-NPs in human bronchial epithelial cells and concluded the intracellular dissolution of these particles was important for their cytotoxicity [22]. However, Gojova *et al.* did not detect the uptake of ZnO-NPs, although they did find that the presence of solid particles was a prerequisite for their cytotoxicity [13, 14].

The objective of this study was to identify the respective contributions of solid particles and released zinc to ZnO-NP cytotoxicity. To this end, we prepared 3 types of exposure media: ZnO-NP suspensions in medium, their extractions collected via centrifugation, and medium containing zinc chloride ($ZnCl_2$), which released the same concentration of zinc as ZnO-NP suspensions in the culture medium. The A549 cell line was used in this study since nanoparticles have been reported to be capable of reaching the alveoli and causing pulmonary inflammation [23, 24]. The A549 cell line is derived from a human lung adenocarcinoma and has been used extensively in airborne particle toxicity studies [12, 25-27] because it maintains most of the characteristics of type II alveolar epithelial cells [28], which play important roles in responding to lung damage and contribute to various pulmonary immunology and inflammatory activities [29].

Materials and methods

1. Preparation and characterization of the exposure media

ZnO-NPs were purchased from Sigma-Aldrich (MO, USA), and $ZnCl_2$ was purchased from WAKO, Ltd., Osaka, Japan. We prepared 3 types of exposure media with these reagents. The first was the suspension: ZnO-NPs were dispersed into sterilized MiliQ water with sonication for 30 min, diluted with Dulbecco's Modified Eagle Medium containing 10% fetal bovine serum (hereafter referred to as supplemented DMEM or medium) to 25, 50, 75, or 100 μg / mL. The hydrodynamic diameter distribution of the ZnO-NP suspension was measured with a laser diffraction particle size analyzer (DLS6000AL, Otsuka Electronics Co., Ltd., Osaka, Japan). The second exposure medium was the extraction: the ZnO-NPs suspensions were incubated in a 37°C, 5% CO_2 incubator for 24 h, and the solid particles were then removed by centrifugation at 150,000 × *g* for 1 h at 4°C. The third exposure medium was $ZnCl_2$ medium: $ZnCl_2$ was dissolved in sterilized MiliQ water and then diluted with medium to the desired concentration. The concentration of the released zinc in the extractions and the $ZnCl_2$ medium was determined with a zinc colorimetric assay kit (AKJ Global Technology Co., Ltd., Chiba, Japan).

2. Cell culture and cytotoxicity assays

A549 cells were seeded in culture dishes with a density of 8,000 cells/cm^2 and incubated for 48 h at 37°C with 5% CO_2. The culture medium was then replaced with 1 of the 3 types of exposure media. After 24 h of exposure, cytotoxicity was assayed through morphological observation with a Cell Double Staining Kit (Dojindo, Kumamoto, Japan), WST cell viability assays using a Cell Counting Kit-8 (CCK-8, Dojindo), and LDH leakage assays using a CytoTox96 Non- radioactive Cytotoxicity Assay Kit (Promega Corporation, Madison, WI, USA). The assays were conducted according to the corresponding kits' protocols.

3. Global gene expression analysis

Total RNA of cells surviving the exposure was extracted with ISOGEN (Nippon Gene Co. Ltd.,

Tokyo, Japan) and purified from the protein and DNA contents with Recombinant DNaseI (Takara Bio, Inc., Shiga, Japan). An Amino Allyl MessageAmp II Arna Amplification Kit (Ambion, TX, USA) was used for the subsequent sample preparation for microarray analysis. We published the sample preparation and scanning procedure previously [30]. Finally, locally weighted scatter plot smoothing (LOWESS) adjustment was applied, and the expression of global genes was transited into corresponding numerical values. Function analysis was conducted via PANTHER's Gene Ontology (GO) biological process categories database (www.pantherdb.org/tools/genexAnalysis.jsp), and the regulated genes were classified into 3 broad functional categories, including "biological process," "cellular function," and "molecular function." Each broad category had a hierarchical structure, and the corresponding genes could be further classified in more detailed functional categories. The function annotation of each gene was calculated with Fisher's exact test to determine the p-value, which represented the statistical significance of the concordance rate between each category and the functional annotation of each gene [31]. Unless the p-value was less than 10^{-4} ($p < 0.0001$), the regulated genes were not considered as an inevitable response to the stress.

4. Inhibiting the expression of the metallothionein gene with siRNA

Lipofectamine™ RNAiMAX (Invitrogen, Carlsbad, CA, USA) was used as a transfection reagent. The transfection mixture was prepared, kept at room temperature for 20 min, and was then added to the cells with the exposure medium. After 24 h of incubation, the cells were collected and used for subsequent cytotoxicity assays or reverse transcription polymerase chain reaction (RT-PCR). For RT-PCR, total RNA was collected with ISOGENE (Nippon Gene Co. Ltd.), purified with Recombinant DNaseI (Takara Bio, Inc.), reverse transcribed into cDNA using a PrimerScript RT reagent kit (Takara Bio, Inc.), and finally stained with LightCycler Fast Start DNA Master SYBR Green I (Roche Applied Science Corp., Germany). The fluorescence intensity was scanned with a LightCycler instrument (CAROUSEL, Roche Applied Science Corp.) and analyzed with corresponding software.

5. Detecting intracellular ROS

The OxiSelect™ Intracellular ROS Assay Kit (Green Fluorescence) was purchased from Cell Biolab, Inc. (CA, USA). The assay kit employed the cell-permeable fluorogenic probe 2′, 7′-dichlorodihydrofluorescin diacetate (DCFH-DA), a well-established reagent for detecting intracellular ROS [32-34]. The exposed cells in opaque 96-well plates were washed twice with DPBS and then incubated in medium containing 100 μM of DCFH-DA at 37°C and 5% CO_2 for 60 min. The fluorescence intensity was then determined with a microplate reader at an excitation of 485 nm and an emission of 530 nm. N-acetyl-L-cysteine (NAC, Sigma-Aldrich), a precursor of intracellular cysteine that can transform into glutathione in cells in order to enhance the intracellular reduction state by increasing the reduced/oxidized glutathione (GSH / GSSG) rate [35], was used to confirm the contribution of ROS to cytotoxicity. A549 cells were pretreated with 10 mM NAC for 2 h, and the medium was then replaced with exposure medium. After another 24-h exposure, cell viability was assayed with the CCK-8 kit.

6. Experimental design and statistical analysis

Unexposed cells were used as a negative control. Each experiment was conducted with 3 parallel samples and repeated independently 3 times. The results were analyzed with 2-tailed Student's t-tests. The results were considered significantly different from the control group if $p < 0.05$.

Results

1. Characterization of ZnO-NP suspensions in supplemented DMEM

We previously reported that the dimensions of ZnO-NPs were less than 60 nm, which is consistent with the nominal dimensions of the particles as determined by the supplier [36]. When the concentrations of the ZnO-NP suspensions ranged from 25 to 100 μg / mL, the mean hydrodynamic diameters of freshly prepared suspensions ranged from 394.7 to 529.3 nm and the mean hydrodynamic diameters ranged from 352.2 to 591.8 nm after incubation or 24 h (Table 1). The concentration of the released zinc in the suspensions was determined using the corresponding extractions and ranged from 6.09 to 9.18 μg / mL; when the particle concentration was more than 75 μg / mL, the released zinc reached the saturation concentration, about 9.18 μg / mL (Table 2).

2. Cytotoxicity of ZnO-NP suspensions, their extractions, and $ZnCl_2$ medium

After A549 cells were exposed to 50, 75, or 100 μg / mL ZnO-NP suspensions for 24 h, cell viability decreased by approximately 20%, 30%, and 60%, respectively, while no change was evident in the case of exposure to 25 μg / mL ZnO-NP suspension (Figure 1a, b). In addition, the LDH leakage assay revealed that exposure to

Table 1 Mean hydrodynamic diameter of ZnO-NPs in supplemented DMEM.

Concentration of ZnO-NPs (μg/mL)	Mean diameter (nm)	
	Freshly prepared medium	24 h-incubated medium
25	525.3	591.8
50	529.3	431.4
75	394.7	449.5
100	406.1	352.2

Abbreviations: DMEM: Dulbecco's Modified Eagle Medium; ZnO-NPs: zinc oxide nanoparticles.

Table 2 Concentration of released zinc in ZnO-NP suspensions.

ZnO-NPs (μg / mL)	Released zinc (μg / mL)
25	6.09
50	7.85
75	9.18
100	9.18

Abbreviation: ZnO-NPs: zinc oxide nanoparticles.

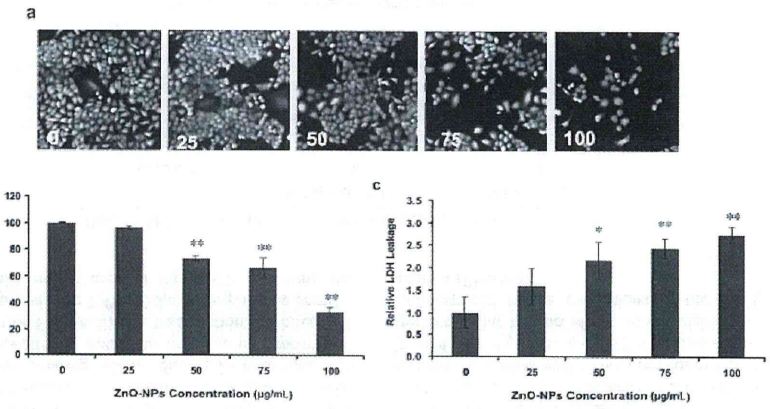

Figure 1 Cytotoxicity induced by ZnO-NP suspensions. A549 cells were exposed to 25, 50, 75, or 100 μg/mL of ZnO-NP suspensions for 24 h, and cell viability was assayed with (a) cell staining, (b) WST, or (c) LDH leakage assay. ** $p < 0.01$, * $p < 0.05$.

Table 3 The number of genes regulated by different treatments.

	ZnO-NP medium 100 μg / mL	$ZnCl_2$ medium 20 μg / mL
Upregulated genes	206	29
Downregulated genes	113	37

Abbreviation: ZnO-NPs: zinc oxide nanoparticles.

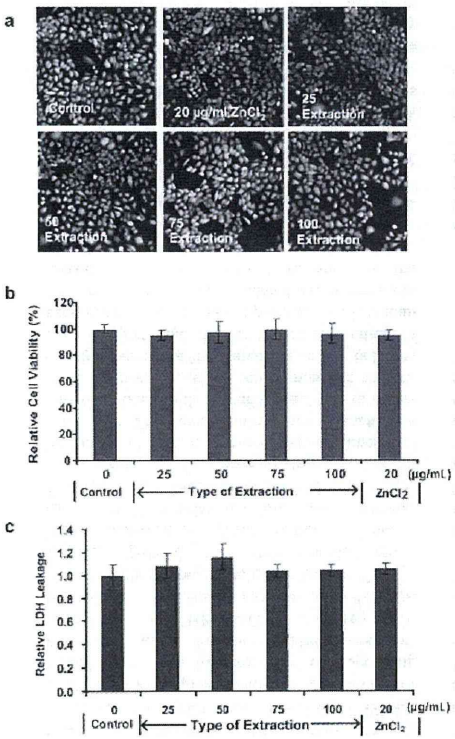

Figure 2 Cytotoxicity induced by 20 μg/mL $ZnCl_2$ or ZnO-NP extraction. A549 cells were exposed to 20 μg/mL $ZnCl_2$ and extractions of the 25, 50, 75, and 100 μg/mL ZnO-NP suspensions for 24 h, and cell viability was assayed with a) cell staining, b) WST, and c) LDH leakage assay. ** $p < 0.01$, * $p < 0.05$.

Table 4 Cadmium ion binding functional category genes regulated by different treatments.

Gene name	Fold change 100 μg / mL ZnO-NPs	Fold change 20 μg / mL $ZnCl_2$
MT1F	5.02	3.53
MT1A	4.90	1.45
MT1B	3.74	1.09
MT1E	3.73	<1.00
MT1L	2.73	<1.00

Abbreviation: ZnO-NPs: zinc oxide nanoparticles.

50, 75, and 100 μg / mL ZnO-NP suspensions also resulted in loss of the integrity of the plasma membrane (Figure 1c). In contrast, zinc released from ZnO-NPs did not cause a reduction in cell viability or have adverse effects on cell number and the integrity of the plasma membrane (Figure 2a-c).

3. Global gene expression analysis

To identify which gene functional categories were regulated in response to ZnO-NPs and released zinc, we conducted cDNA microarray analysis of cells exposed to 100 μg / mL ZnO-NP suspension or 20 μg / mL $ZnCl_2$. We used 20 μg / mL $ZnCl_2$ as the released zinc control in the absence of the solid particles to avoid possible interference from released impurities in the extractions and because we found that medium treated with 20 μg / mL $ZnCl_2$ contained about 10 μg/mL released zinc (data not shown), which was equivalent to that of the 100 μg / mL ZnO-NP suspension. In response to the 100 μg / mL ZnO-NP suspension, 206 and 113 genes were up- or downregulated, respectively; in contrast, in response to 20 μg / mL $ZnCl_2$ medium, 29 and 37 genes were up- or downregulated, respectively (Table 3 and Table S1–S4). Through the subsequent data mining on the regulated genes via PANTHER's GO biological process categories database, the same functional gene category, "cadmium ion binding," was identified in response to both the ZnO-NP suspension and the $ZnCl_2$ treatment. The "cadmium ion binding" category consisted of 5 MT isomer genes: MT1F, MT1A, MT1B, MT1E, and MT1L. The fold change of MT expression is summarized in Table 4. No significantly changed functional category was identified among the downregulated genes.

4. Cytotoxicity in the absence of MT overexpression

To confirm the role of MT in ZnO-NP-induced cytotoxicity, we inhibited MT expression with corresponding siRNA during 24-h exposure to ZnO-NPs or $ZnCl_2$. In the case of exposure to ZnO-NPs, the siRNA transfection inhibited MT expression to 1.4% of the corresponding control, while in the case of the $ZnCl_2$ exposure, the siRNA transfection inhibited the MT expression to 1.1% of the corresponding control (Table 5). We then assayed cell viability. Inhibiting MT expression resulted in a decrease in cell viability to about 88%, 80%, and 53% of the control in 50, 75, and 100 μg / mL ZnO-NP suspensions, respectively, but had no effect on the viability of cells exposed to the extractions or the $ZnCl_2$ medium (Figure 3).

Table 5 MT1F inhibition efficiency of MT isomer gene expression.

	100 μg / mL ZnO-NPs	20 μg / mL $ZnCl_2$
Control [a]	1	1
MTs siRNA	0.014	0.011

[a]The expression of MTs in cells transfected with a random RNA sequence was used as a control, and the expression of MT in cells transfected with MT siRNA was calculated to be a portion of the control. Abbreviations: ZnO-NPs: zinc oxide nanoparticles; MT: metallothionein.

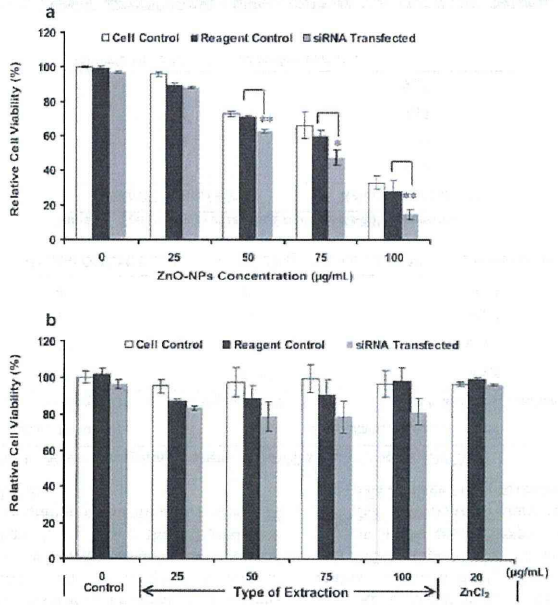

Figure 3 Function of MTs in response to the various exposures. MT expression in A549 cells was inhibited with corresponding siRNA during exposure to (a) suspensions of 25, 50, 75, or 100 μg/mL ZnO-NPs or (b) their extractions or 20 μg/mL $ZnCl_2$ for 24 h. Cell viability was assayed with WST. The statistical significance was analyzed by comparing siRNA-transfected cells with corresponding reagent controls. ** $p < 0.01$, * $p < 0.05$.

5. Intracellular ROS

Intracellular ROS was detected when ZnO-NPs were more than 50 μg/mL; however, no ROS generation was observed in the cells exposed to $ZnCl_2$ (Figure 4). To examine whether ROS induced by ZnO-NPs was involved in cytotoxicity, cells were pretreated with NAC before exposure to ZnO-NPs. As shown in Figure 5, cell viability was partially recovered by NAC treatment in cells treated with 50 μg / mL and 75 μg/mL ZnO-NPs. However, in the case of the 100 μg / mL ZnO-NP suspension, NAC pretreatment had no effect on the cell viability.

6. Synergic toxicity of ROS and zinc

Next, we incubated A549 cells in the exposure medium containing $ZnCl_2$ and / or H_2O_2 for 24 h. According to the concentration of H_2O_2, exposure media were designed as 0 mM, 0.5 mM, and 1 mM; in each group, the concentration of $ZnCl_2$ ranged from 0 to 50 μg / mL. Cell viability was assayed after a 24-h incubation. As shown in Figure 6, in absence of H_2O_2, 20 μg / mL $ZnCl_2$ had no effect on cell viability; however, in presence of 0.5 or 1 mM H_2O_2, 20 μg / mL $ZnCl_2$ reduced cell viabilities to about 83% and 50% of the control, respectively. In the case of 30 μg / mL $ZnCl_2$, there was no change in cell viability in absence of H_2O_2, while in presence of 0.5 or 1 mM of H_2O_2, cell viability decreased to 75% and 10%, respectively. Treatment with 40 μg / mL $ZnCl_2$ resulted in a decrease in relative cell viability to 0 in presence of 1 mM H_2O_2, but decreased cell viability by only about 15% in the absence of H_2O_2 and by about 40% in the presence of 0.5 mM H_2O_2.

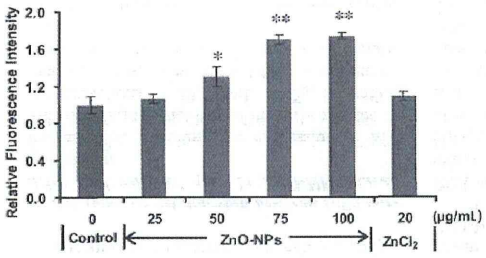

Figure 4 The intracellular ROS assay with DCFH-DA. The fluorescence intensity is directly proportional to the intracellular ROS concentration. ** $p < 0.01$, * $p < 0.05$.

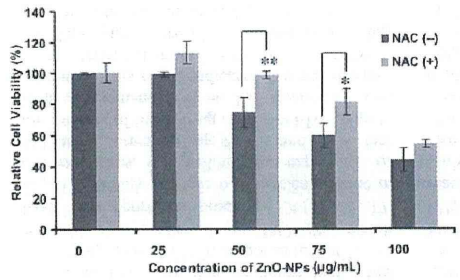

Figure 5 Changes in cell viability after NAC pre-incubation. After pre- incubated with NAC for 2 h, A549 cells were exposed to ZnO-NPs for another 24 h, and cell viability was assayed with WST. ** $p < 0.01$, * $p < 0.05$.

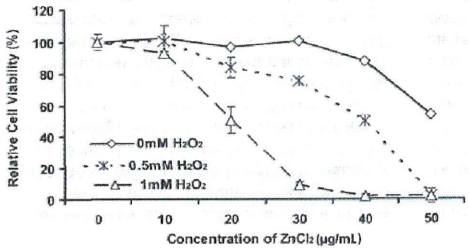

Figure 6 The synergic effect of H_2O_2 and zinc. The results are presented as the percentage of the control (0 mM $ZnCl_2$) of the corresponding group. The statistical significance of the change in cell viability was analyzed by comparing with the control series.

Discussion

1. The exposure design

The dissolution of zinc oxide is a well-described phenomenon that occurs over a wide range of pH values [37]. In water at pH 7.5, the overall dissolution reaction of zinc oxide can be shortly written as follows: ZnO (s) ⇌ Zn2+ (aq) + OH (aq) [38, 39]. Franklin *et al.* discussed the importance of the water solubility of ZnO-NPs in their toxicity study on microalga [20]. However, in previous studies, the solubility and saturation of ZnO-NPs in different culture media were rarely taken into consideration, which resulted in ZnO-NP cytotoxicity being compared with the toxicity of zinc salt consisting of the equivalent moles of zinc rather than zinc salt with the same capability to release zinc in the solvent [18, 22, 40]. This introduces the risk of not accurately estimating true exposure and the possibility of over- or underestimating the effects of the released zinc. Since the objective of this study was to identify the respective contributions of released zinc and solid particles on the cytotoxicity of ZnO-NPs, we used ZnO-NP extractions to control for the zinc released from the ZnO-NP suspension in the cytotoxicity assay.

For the global gene expression analysis, we used $ZnCl_2$ medium as the released zinc control to avoid potential interference from impurities in the extractions. We measured the concentration of released zinc in the ZnO-NP suspensions and $ZnCl_2$ medium using a zinc-specific chelator [41] and found that the released zinc in 100 μg/mL of the ZnO-NP suspension reached the saturation concentration, about 9.18 μg / mL, which was equivalent to the zinc concentration in 20 μg / mL of $ZnCl_2$ medium. Therefore, we used the 20 μg / mL $ZnCl_2$ medium concentration as a control for the released zinc from the 100 μg / mL ZnO-NP suspension in our gene expression analysis. Additionally, using the saturation zinc concentration of the ZnO-NPs, we could avoid the potential interference of the "bound zinc/free zinc" ratio induced by different solubilities since this issue has not been studied clearly [42-44]. Bound zinc and free zinc are different forms of released zinc in supplemented DMEM. The zinc binding capacity of DMEM has garnered concerns in *in vitro* studies. Part of the total zinc is localized by zinc ligands in DMEM; therefore, the total released zinc can be separated into 2 groups: free zinc and bound zinc, which binds to protein components in the medium [45, 46]. Here, we attempted to address this problem by measuring the total released zinc using a zinc-specific chelator. However, we are continuing to work on this issue since the effects of free zinc and bound zinc on *in vitro* toxicity have not been fully elucidated [17].

2. Both solid particles and released zinc contribute to ZnO-NP-dependent cytotoxicity

With the above modification, we found that the ZnO-NP suspension reduced the cell viability, damaged the integrity of the plasma membrane, and induced abnormal cell morphologies; however, neither the extractions nor the $ZnCl_2$ medium showed adverse effects on A549 cells. These findings indicated the importance of solid particles for ZnO-NP-induced cytotoxicity and are consistent with the predictions of Moos *et al.*, who hypothesized that the presence of solid particles was necessary for ZnO-NP-induced cytotoxicity [14].

Our subsequent global gene expression analysis revealed that the same functional category, "cadmium ion binding," was upregulated in response not only to $ZnCl_2$, but also to ZnO-NPs, despite the fact that these 2 treatments exhibited the opposite effects on exposed cells (nontoxic and toxic, respectively). The "cadmium ion binding" category consisted of MTs that belong to the well-studied cysteine-rich metalloprotein family. MTs play important roles in maintaining the intracellular homeostasis of heavy metals via binding, exchanging, and transporting heavy metals, such as zinc, cadmium, and copper, with their cysteine residues [47, 48]. For example, when cells are suddenly exposed to high levels of zinc, apo-MTs capture

excessive intracellular zinc, reducing it to non-toxic levels, while the cells upregulate the expression of MTs via metal regulatory transcription factor 1 (MTF1)-mediated feedback [49]. Additionally, MTs are also reported to act as intracellular antioxidants to quench ROS in some special cases [50]. In the current study, we exposed A549 cells to medium containing H_2O_2 and found no change in the expression of MT. Accordingly, we could rule out the possibility that the overexpression of MTs occurred in response to ROS and thus proposed that A549 cells upregulated MTs in response to $ZnCl_2$ and released zinc generated by ZnO-NPs, which have been reported to produce ROS[12, 16, 17, 22]. To identify the role of the released zinc in our exposures, we inhibited the expression of MT using corresponding siRNA and found that the toxicity of the 100 μg / mL ZnO-NP suspension was enhanced when MT expression was inhibited. This result indicated that the released zinc contributed to ZnO-NP-induced cytotoxicity. The cytotoxicity of the excessive zinc has been reported to inhibit cellular respiration [51, 52] and the key enzymes in the glycolytic pathway, leading to ATP depletion in cells [53, 54].

3. The synergic relationship between solid particles and released zinc in ZnO-NP-induced cytotoxicity

Interestingly, inhibiting the expression of MT did not affect the viability of the cells exposed to the extractions or 20 μg/mL $ZnCl_2$, indicating that the released zinc did not have a substantial effect on the cells in the absence of solid particles.

The "Trojan-horse" theory has been likened to the role of solid particles in ZnO-NPs: nanoparticles bring zinc ions into cells through particle internalization by cells, similar to how the Greeks were brought into the city of Troy by the wooden horse, leading to adverse effects and even cell death [21, 40]. Although one report has demonstrated the internalization of ZnO-NPs by A549 cells [12], no data has yet demonstrated the proportional correlation of uptake and cytotoxicity. In this study, we also observed exposed cells and rarely found endocytosis of the particles by A549 cells (data not shown). The other possibility is that the particles generate ROS, since ROS is thought to be the most important mechanism of nanotoxicity [55]. With DCFH, we detected intracellular ROS following exposure to ZnO-NPs, but not following exposure to the $ZnCl_2$ medium. Furthermore, when we pretreated A549 cells with NAC, a precursor of intracellular antioxidants, cell viability was recovered, unlike in untreated cells. Thus, we concluded that ROS contributed to ZnO-NP-induced cytotoxicity via solid particles.

In the case of the nanoparticles of transient metal oxides, such as copper oxide (CuO-NPs) and iron oxide, ROS is thought to be produced by the dissolved metal ions via Fenton's reaction [21, 22]. However, divalent zinc is not redox reactive and is not usually thought to cause Fenton's reaction [19, 56]. In a previous study, we also demonstrated the different toxic behaviors of a typical transient metal oxide, CuO-NPs, and a semiconductive material, ZnO-NPs [36]. The oxidation potential of ZnO nanomaterial has been attributed to its unique surface properties resulting from the quantum size of the particles [1, 57-59]. Thus, we propose the special surface reactivity of ZnO-NPs is the reason for the necessity of the solid particles in ZnO-NP-dependent cytotoxicity.

To demonstrate the relationship between ROS and released zinc in ZnO-NP-induced cytotoxicity, we exposed A549 cells to $ZnCl_2$ and H_2O_2 simultaneously. We found that the toxicity of released zinc was enhanced by H_2O_2, similar to a report by Heng *et al.* demonstrating that the cytotoxicity of ZnO-NPs was aggravated by exogenous ROS [15]. Zhang explained that ROS could incapacitate MTs via oxidation of sulfhydryl groups, leading to an increase in intracellular free zinc to toxic levels [60]. We propose that the solid particles produce ROS via their special surface activity, and the generated ROS can then incapacitate MT, the most important protein involved in maintaining intracellular zinc homeostasis, finally allowing intracellular free zinc to reach toxic levels.

The findings of this study indicated that both solid particles and released zinc contribute to the cytotoxicity of ZnO-NPs, while released zinc alone does not cause substantial toxicity in A549 cells in the absence of solid particles. Moreover, we propose that released zinc and

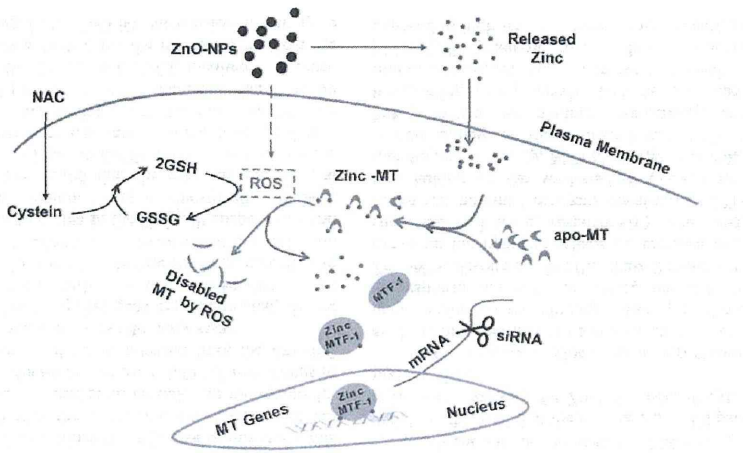

Figure 7 Synergic toxicity of solid particles and released zinc from ZnO-NPs in A549 cells. Once dispersed into the cell culture medium, ZnO-NPs release zinc and generate ROS. To maintain the homeostasis of intracellular free zinc, A549 cells upregulate the expression of apo-MTs via the zinc-MTF1 complex. ROS not only destroy the intracellular redox status, they also oxidize the MTs, resulting in the zinc defense breakdown.

solid particles have a synergistic effect on toxicity as follows: in response to the excessive released zinc generated by ZnO-NPs, A549 cells upregulate the expression of MT; the solid particles produce ROS via their special surface chemical reactions and inhibit MT, thereby leading to the breakdown of the defense against the excessive intracellular free zinc (Figure 7).

Nowadays, human exposure to engineered nanoparticles is inevitable since nanoparticles are becoming more and more widely used. Our previous knowledge of airborne pollutant particles, such as diesel exhaust, provides important details on the toxicology of ultrafine particles (<100 nm), especially in established ROS models for toxicological mechanisms of particulate materials [61]. However, unlike the similarity with airborne pollutant particles, engineered nanomaterials have physicochemical properties distinct to their different chemical compositions. Thus, we must consider true exposure to nanomaterials on a case-by-case basis to determine cytotoxicity to each biological system, and this will become very important in evaluating the toxic potential of nanoparticles and improving engineered nanomaterials. We also suggest that both the nanoscaled superficial properties and the dissolved chemical composition of nanosized metal oxides should be characterized fully. Moreover, the synergic effects of these particles should be determined in future studies.

Acknowledgments

We would like to thank Ms. H. Morita and Dr. T. Takemura for technical assistance. This work was supported by a Grant-in-Aid from the Ministry of Health, Labour, and Welfare of Japan.

References

1) Fan Z, Lu J G. Zinc oxide nanostructures: synthesis and properties. J Nanosci Nanotechnol 2005; 5: 1561-1573.
2) Djurišić A B, Leung Y H. Optical properties of ZnO nanostructures. Small 2006; 2: 944-961.
3) Banerjee D, Lao J Y, Wang D Z, Huang J Y, Steeves D, Kimball B, Ren Z F. Synthesis and photoluminescence studies on ZnO nanowires. Nanotechnology 2004; 15: 404-409.
4) De Berardis B, Civitelli G, Condello M, Lista P, Pozzi R, Arancia G, Meschini S. Exposure to ZnO nanoparticles induces oxidative stress and cytotoxicity in human colon carcinoma cells.

Toxicol Appl Pharmacol 2010.[Epub ahead of print]
5) Ostrowski A D, Martin T, Conti J, Hurt I, Harthorn B H. Nanotoxicology: characterizing the scientific literature, 2000-2007. J Nanopart Res 2009; 11: 251-257.
6) OECD. Guidance Manual for the Testing of Manufactured Nanomaterials: OECD's Sponsorship Programme. 2009.
7) Zhu X S, Zhu L, Duan Z H, Qi R Q, Li Y, Lang Y P. Comparative toxicity of several metal oxide nanoparticle aqueous suspensions to Zebrafish (Danio rerio) early developmental stage. J Environ Sci Heal A 2008; 43: 278-284.
8) Wiench K, Wohlleben W, Hisgen V, Radke K, Salinas E, Zok S, Landsiedel R. Acute and chronic effects of nano- and non-nano-scale TiO(2) and ZnO particles on mobility and reproduction of the freshwater invertebrate Daphnia magna. Chemosphere 2009; 76: 1356-1365.
9) Lin D H, Xing B S. Phytotoxicity of nanoparticles: Inhibition of seed germination and root growth. Environ Pollut 2007; 150: 243-250.
10) Jones N, Ray B, Ranjit K T, Manna A C. Antibacterial activity of ZnO nanoparticle suspensions on a broad spectrum of microorganisms. FEMS Microbiol Lett 2008; 279: 71-76.
11) Jeng H A, Swanson J. Toxicity of metal oxide nanoparticles in mammalian cells. J Environ Sci Heal A 2006; 41: 2699-2711.
12) Lin W S, Xu Y, Huang C C, Ma Y F, Shannon K B, Chen D R, Huang Y W. Toxicity of nano- and micro-sized ZnO particles in human lung epithelial cells. J Nanoparticle Res 2009; 11: 25-39.
13) Gojova A, Guo B, Kota R S, Rutledge J C, Kennedy I M, Barakat a I. Induction of inflammation in vascular endothelial cells by metal oxide nanoparticles: effect of particle composition. Environ Health Perspect 2007; 115: 403-409.
14) Moos P J, Chung K, Woessner D, Honeggar M, Cutler N S, Veranth J M. ZnO Particulate Matter Requires Cell Contact for Toxicity in Human Colon Cancer Cells. Chem Res Toxicol 2010; 23: 733-739.
15) Heng B C, Zhao X X, Xiong S J, Ng K W, Boey F Y C, Loo J S C. Toxicity of zinc oxide (ZnO) nanoparticles on human bronchial epithelial cells (BEAS-2B) is accentuated by oxidative stress. Food Chem Toxicol 2010; 48: 1762-1766.
16) Sharma V, Shukla R K, Saxena N, Parmar D, Das M, Dhawan A. DNA damaging potential of zinc oxide nanoparticles in human epidermal cells. Toxicol Lett 2009; 185: 211-218.
17) Yin H, Casey P S, Mccall M J, Fenech M. Effects of surface chemistry on cytotoxicity, genotoxicity, and the generation of reactive oxygen species induced by ZnO nanoparticles. Langmuir 2010; 26: 15399-15408.
18) Brunner T J, Wick P, Manser P, Spohn P, Grass R N, Limbach L K, Bruinink A, Stark W J. In vitro cytotoxicity of oxide nanoparticles: comparison to asbestos, silica, and the effect of particle solubility. Environ Sci Technol 2006; 40: 4374-4381.
19) Eigen M. Fast elementary steps in chemical reaction mechanisms. Pure Appl Chem 1963; 6: 97-116.
20) Franklin N M, Rogers N J, Apte S C, Batley G E, Gadd G E, Casey P S. Comparative toxicity of nanoparticulate ZnO, bulk ZnO, and ZnCl2 to a freshwater microalga (Pseudokirchneriella subcapitata): the importance of particle solubility. Environ Sci Technol 2007; 41: 8484-8490.
21) Limbach L K, Wick P, Manser P, Grass R N, Bruinink A, Stark W J. Exposure of engineered nanoparticles to human lung epithelial cells: Influence of chemical composition and catalytic activity on oxidative stress. Environ Sci Technol 2007; 41: 4158-4163.
22) Xia T, Kovochich M, Liong M, Madler L, Gilbert B, Shi H B, Yeh J I, Zink J I, Nel A E. Comparison of the mechanism of toxicity of zinc oxide and cerium oxide nanoparticles based on dissolution and oxidative stress properties. ACS Nano 2008; 2: 2121-2134.
23) Heyder J. Deposition of inhaled particles in the human respiratory tract and consequences for regional targeting in respiratory drug delivery. Proc Am Thorac Soc 2004; 1: 315-320.
24) Muhlfeld C, Rothen-Rutishauser B, Blank F, Vanhecke D, Ochs M, Gehr P. Interactions of nanoparticles with pulmonary structures and cellular responses. Am J Physiol Lung Cell Mol Physiol 2008; 294: L817-829.
25) Singh S, Shi T, Duffin R, Albrecht C, Van Berlo D, Hohr D, Fubini B, Martra G, Fenoglio I, Borm P J, Schins R P. Endocytosis, oxidative stress and IL-8 expression in human lung epithelial cells upon treatment with fine and ultrafine TiO2: role of the specific surface area and of surface methylation of the particles. Toxicol Appl Pharmacol 2007; 222: 141-151.
26) Kim J S, Yoon T J, Yu K N, Noh M S, Woo M, Kim B G, Lee K H, Sohn B H, Park S B, Lee J K, Cho M H. Cellular uptake of magnetic nanoparticle is mediated through energy-dependent endocytosis in A549 cells. J Vet Sci 2006; 7: 321-326.
27) Stringer B, Kobzik L. Environmental particulate-mediated cytokine production in lung epithelial cells (A549): role of preexisting inflammation and oxidant stress. J Toxicol Env Heal A 1998; 55: 31-44.
28) Foster K A, Oster C G, Mayer M M, Avery M L, Audus K L. Characterization of the A549 cell line as a type II pulmonary epithelial cell model for drug metabolism. Exp Cell Res 1998; 243: 359-366.
29) Thompson A B, Robbins R A, Romberger D J, Sisson J H, Spurzem J R, Teschler H, Rennard S I. Immunological functions of the pulmonary epithelium. Eur Respir J 1995; 8: 127-149.
30) Hanagata N, Zhuang F, Connolly S, Li J, Ogawa N, Xu M S. Molecular responses of human lung epithelial cells to the toxicity of copper oxide nanoparticles inferred from whole genome expression analysis. ACS Nano 2011; 5: 9326-9338.
31) Hosack D A, Dennis G, Sherman B T, Lane H C, Lempicki R A. Identifying biological themes within lists of genes with EASE. Genome Biol 2003; 4.
32) Keller A, Mohamed A, Drose S, Brandt U, Fleming I, Brandes R P. Analysis of dichlorodihydrofluorescein and dihydrocalcein as probes for the detection of intracellular reactive oxygen species. Free Radical Res 2004; 38: 1257-1267.
33) Halliwell B, Whiteman M. Measuring reactive species and oxidative damage in vivo and in cell culture: how should you do it and what do the results mean? Brit J Pharmacol 2004; 142: 231-255.
34) Wang H, Joseph J A. Quantifying cellular oxidative stress by dichlorofluorescein assay using microplate reader. Free Radic Biol Med 1999; 27: 612-616.
35) Kowaltowski A J, Vercesi a E. Mitochondrial damage induced by conditions of oxidative stress. Free Radic Biol Med 1999; 26: 463-471.
36) Xu M S, Fujita D, Kajiwara S, Minowa T, Li X L, Takemura T, Iwai H, Hanagata N. Contribution of physicochemical characteristics of nano-oxides to cytotoxicity. Biomaterials 2010; 31: 8022-8031.
37) Bian S W, Mudunkotuwa I A, Rupasinghe T, Grassian V H. Aggregation and dissolution of 4 nm ZnO nanoparticles in aqueous environments: influence of pH, ionic strength, size, and adsorption of humic acid. Langmuir 2011; 27: 6059-6068.
38) Degen A, Kosec M. Effect of pH and impurities on the surface charge of zinc oxide in aqueous solution. J Eur Ceramic Soc 2000; 20: 667-673.
39) Yamabi S, Imai H. Growth conditions for wurtzite zinc oxide films in aqueous solutions. J Mater Chem 2002; 12: 3773-3778.
40) Deng X Y, Luan Q X, Chen W T, Wang Y L, Wu M H, Zhang H J, Jiao Z. Nanosized zinc oxide particles induce neural stem cell apoptosis. Nanotechnol 2009; 20.
41) Makino T, Saito M, Horiguchi D, Kina K. A highly sensitive colorimetric determination of serum zinc using water-soluble pyridylazo dye. Clin Chim Acta 1982; 120: 127-135.
42) Bai W, Zhang Z Y, Tian W J, He X, Ma Y H, Zhao Y L, Chai Z F. Toxicity of zinc oxide nanoparticles to zebrafish embryo: a physicochemical study of toxicity mechanism. J Nanoparticle Res 2010; 12: 1645-1654.
43) Nel A E, Madler L, Velegol D, Xia T, Hoek E M V, Somasundaran P, Klaessig F, Castranova V, Thompson M. Understanding biophysicochemical interactions at the nano-bio interface. Nat Mater 2009; 8: 543-557.
44) Cedervall T, Lynch I, Lindman S, Berggard T, Thulin E, Nilsson H, Dawson K A, Linse S. Understanding the nanoparticle-protein corona using methods to quantify exchange rates and affinities of proteins for nanoparticles. Proc Nat Acad Sci U S A 2007; 104: 2050-2055.
45) Bozym R A, Chimienti F, Giblin L J, Gross G W, Korichneva I, Li Y A, Libert S, Maret W, Parviz M, Frederickson C J, Thompson R B. Free zinc ions outside a narrow concentration range are toxic to a variety of cells in vitro. Exp Biol Med 2010; 235: 741-750.
46) Lu J, Stewart a J, Sadler P J, Pinheiro T J T, Blindauer C A. Albumin as a zinc carrier: properties of its high-affinity zinc-binding site. Biochem Soc Trans 2008; 36: 1317-1321.
47) Guan Y S. Comments to metallothionein as an anti-inflammatory mediator. Mediat Inflamm 2009.
48) Inoue K I, Takano H, Shimada A, Satoh M. Metallothionein as an anti-inflammatory mediator. Mediat Inflamm 2009.
49) Gyulkhandanyan A V, Lee S C, Bikopoulos G, Dai F H, Wheeler M B. The Zn2+-transporting pathways in pancreatic beta-cells - a role for the L-type voltage-gated Ca2+ channel. J Biol Chem 2006; 281: 9361-9372.
50) Vliagoftis A, Schwingshackl A, Milne C D, Duszyk M, Hollenberg M D, Wallace J L, Befus A D, Moqbel R. Proteinase-activated receptor-2-mediated matrix metalloproteinase-9 release from airway epithelial cells. J Allergy Clin Immun 2000; 106: 537-545.
51) Sensi S L, Yin H Z, Carriedo S G, Rao S S, Weiss J H. Preferential Zn2+ influx through Ca2+-permeable AMPA/kainate channels triggers prolonged mitochondrial superoxide production. Proc Nat Acad Sci U S A 1999; 96: 2414-2419.
52) Frazzini V, Rockabrand E, Mocchegiani E, Sensi S L. Oxidative stress and brain aging: is zinc the link? Biogerontology 2006; 7: 307-314.
53) Dineley K E, Votyakova T V, Reynolds I J. Zinc inhibition of cellular energy production: implications for mitochondria and neurodegeneration. J Neurochem 2003; 85: 563-570.
54) Gazaryan I G, Krasinskaya I P, Kristal B S, Brown A M. Zinc irreversibly damages major enzymes of energy production and antioxidant defense prior to mitochondrial permeability

transition. J Biol Chem 2007; 282: 24373-24380.
55) Nel A, Xia T, Madler L, Li N. Toxic potential of materials at the nanolevel. Science 2006; 311: 622-627.
56) Nakamura M, Shishido N, Nunomura A, Smith M A, Perry G, Hayashi Y, Nakayama K, Hayashi T. Three histidine residues of amyloid-beta peptide control the redox activity of copper and iron. Biochemistry 2007; 46: 12737-12743.
57) Wang X D, Ding Y, Summers C J, Wang Z L. Large-scale synthesis of six-nanometer-wide ZnO nanobelts. J Phys Chem B 2004; 108: 8773-8777.
58) Kukreja L M, Barik S, Misra P. Variable band gap ZnO nanostructures grown by pulsed laser deposition. J Cryst Growth 2004; 268: 531-535.
59) Chiou J W, Kumar K P K, Jan J C, Tsai H M, Bao C W, Pong W F, Chien F Z, Tsai M H, Hong I H, Klauser R, Lee J F, Wu J J, Liu S C. Diameter dependence of the electronic structure of ZnO nanorods determined by x-ray absorption spectroscopy and scanning photoelectron microscopy. Appl Phys Lett 2004; 85: 3220-3222.
60) Zhang B, Georgiev O, Hagmann M, Gunes C, Cramer M, Faller P, Vasak M, Schaffner W. Activity of metal-responsive transcription factor 1 by toxic heavy metals and H2O2 in vitro is modulated by metallothionein. Mol Cell Biol 2003; 23: 8471-8485.
61) Li N, Sioutas C, Cho A, Schmitz D, Misra C, Sempf J, Wang M, Oberley T, Froines J, Nel A. Ultrafine particulate pollutants induce oxidative stress and mitochondrial damage. Environ Health Perspect 2003; 111: 455-460.

(Received: November 15, 2012/
Accepted: December 20, 2012)

Corresponding author:
Nobuttaka HANAGATA, Ph.D.
Nanotechnology Innovation Station,
National Institute for Materials Science (NIMS)
1-2-1 Sengen, Tsukuba, Ibaraki 305-0047, Japan
Tel: +81-29-860-4774 Fax: +81-29-859-2475
E-mail: HANAGATA.Nobutaka@nims.go.jp

Table S1 List of the Genes Up-regulated by 100 μg / mL of ZnO-NPs in A549 cells.

Gene symbol	Description	Fold change
MT1F	Homo sapiens metallothionein 1F (MT1F), mRNA [NM_005949]	5.02
MT1A	Homo sapiens metallothionein 1A (MT1A), mRNA [NM_005946]	4.99
MT1G	Homo sapiens metallothionein 1G (MT1G), mRNA [NM_005950]	4.31
LOC387763	Protein Ag2 homolog [Source:UniProtKB/Swiss-Prot;Acc:Q7Z7L8] [ENST00000339446]	4.29
MT2A	Homo sapiens metallothionein 2A (MT2A), mRNA [NM_005953]	3.93
IL1F7	Homo sapiens interleukin 1 family, member 7 (zeta) (IL1F7), transcript variant 1, mRNA [NM_014439]	3.90
MT1B	Homo sapiens metallothionein 1B (MT1B), mRNA [NM_005947]	3.74
MT1E	Homo sapiens metallothionein 1E (MT1E), mRNA [NM_175617]	3.73
EGR1	Homo sapiens early growth response 1 (EGR1), mRNA [NM_001964]	3.72
MT1X	Homo sapiens metallothionein 1X (MT1X), mRNA [NM_005952]	3.60
PTPRR	Homo sapiens protein tyrosine phosphatase, receptor type, R (PTPRR), transcript variant 1, mRNA [NM_002849]	3.51
SUSD5	Homo sapiens sushi domain containing 5 (SUSD5), mRNA [NM_033551]	3.40
SLC30A2	Homo sapiens solute carrier family 30 (zinc transporter), member 2 (SLC30A2), transcript variant 1, mRNA [NM_001004434]	3.30
MT1H	Homo sapiens metallothionein 1H (MT1H), mRNA [NM_005951]	3.11
HSPA6	Homo sapiens heat shock 70kDa protein 6 (HSP70B') (HSPA6), mRNA [NM_002155]	3.02
MT1L	Homo sapiens metallothionein 1L (gene/pseudogene) (MT1L), non-coding RNA [NR_001447]	2.73
ATF3	Homo sapiens activating transcription factor 3 (ATF3), transcript variant 4, mRNA [NM_001030619]	2.41
HEX2	Homo sapiens brain expressed X-linked 2 (HEX2), mRNA [NM_013621]	2.34
STK33	Homo sapiens serine/threonine kinase 33 (STK33), mRNA [NM_030906]	2.34
DHRS2	Homo sapiens dehydrogenase/reductase (SDR family) member 2 (DHRS2), transcript variant 1, mRNA [NM_182908]	2.31
BEX4	Homo sapiens brain expressed, X-linked 4 (BEX4), mRNA [NM_001127688]	2.29
PAQR7	Homo sapiens progestin and adipoQ receptor family member VII (PAQR7), mRNA [NM_173425]	2.27
ARC	Homo sapiens activity-regulated cytoskeleton-associated protein (ARC), mRNA [NM_015193]	2.20
SERTAD1	Homo sapiens SERTA domain containing 1 (SERTAD1), mRNA [NM_019601]	2.19
KRT34	Homo sapiens keratin 34 (KRT34), mRNA [NM_021013]	2.13
ARVCF	Homo sapiens armadillo repeat gene deletes in velocardiofacial syndrome (ARVCF), mRNA [NM_001670]	2.12
PSPN	Homo sapiens persephin (PSPN), mRNA [NM_003158]	2.05
EMP1	Homo sapiens epithelial membrane protein 1 (EMP1), mRNA [NM_001423]	1.99
MXD1	Homo sapiens MAX dimerization protein 1 (MXD1), mRNA [NM_002357]	1.98
KLRC3	Homo sapiens killer cell lectin-like receptor subfamily C, member 3 (KLRC3), transcript variant 2, mRNA [NM_007333]	1.97
SLC30A1	Homo sapiens solute carrier family 30 (zinc transporter), member 1 (SLC30A1), mRNA [NM_021194]	1.96
DUSP8	Homo sapiens dual specificity phosphatase 8 (DUSP8), mRNA [NM_004420]	1.92
MMP1	Homo sapiens matrix metallopeptidase 1 (interstitial collagenase) (MMP1), mRNA [NM_002421]	1.91
LOC221710	Homo sapiens hypothetical protein LOC221710 (LOC221710), mRNA [NM_001135575]	1.90
SLC04A1	Homo sapiens solute carrier organic anion transporter family, member 4A1 (SLCO4A1), mRNA [NM_016354]	1.88
NPL	Homo sapiens N-acetylneuraminate pyruvate lyase (dihydrodipicolinate synthase) (NPL), mRNA [NM_020994]	1.84
SLFN5	Homo sapiens schlafen family member 5 (SLFN5), mRNA [NM_144975]	1.82
KLRC1	Homo sapiens killer cell lectin-like receptor subfamily C, member 1 (KLRC1), transcript variant 1, mRNA [NM_002259]	1.80
RFPL2	Homo sapiens ret finger protein-like 2 (RFPL2), transcript variant 1, mRNA [NM_006693]	1.78
CAMTA1	Homo sapiens calmodulin binding transcription activator 1 (CAMTA1), mRNA [NM_015215]	1.77
FOSB	Homo sapiens FBJ murine osteosarcoma viral oncogene homolog B (FOSB), transcript variant 1, mRNA [NM_006732]	1.77
LOC100129113	Homo sapiens cDNA FLJ37134 fis, clone BRACE2026293 [AK094477]	1.77

Gene symbol	Description	Fold-change
KLRC2	Homo sapiens killer cell lectin-like receptor subfamily C, member 2 (KLRC2), mRNA [NM_002260]	1.77
ZNF365	Homo sapiens zinc finger protein 365 (ZNF365), transcript variant A, mRNA [NM_014951]	1.76
ENG	Homo sapiens endoglin (ENG), transcript variant 2, mRNA [NM_000118]	1.74
CCNG2	Homo sapiens cyclin G2 (CCNG2), mRNA [NM_004354]	1.73
IL11	Homo sapiens interleukin 11 (IL11), mRNA [NM_000641]	1.73
MYBL1	Homo sapiens v-myb myeloblastosis viral oncogene homolog (avian)-like 1 (MYBL1), mRNA [NM_001080416]	1.71
C17orf67	Homo sapiens chromosome 17 open reading frame 67 (C17orf67), mRNA [NM_001085430]	1.71
NEFL	Homo sapiens neurofilament, light polypeptide (NEFL), mRNA [NM_006158]	1.67
DNER	Homo sapiens delta/notch-like EGF repeat containing (DNER), mRNA [NM_139072]	1.66
MT1F	Homo sapiens MT1F (MT1F) mRNA, complete cds [AF348594]	1.66
TMEM158	Homo sapiens transmembrane protein 158 (TMEM158), mRNA [NM_015444]	1.64
RGS16	Homo sapiens regulator of G-protein signaling 16 (RGS16), mRNA [NM_002928]	1.61
NEK7	Homo sapiens NIMA (never in mitosis gene a)-related kinase 7 (NEK7), mRNA [NM_133494]	1.62
CCNG2	Homo sapiens cyclin G2 (CCNG2), mRNA [NM_004354]	1.61
BARHL1	Homo sapiens BarH-like homeobox 1 (BARHL1), mRNA [NM_020064]	1.60
FAM129A	Homo sapiens family with sequence similarity 129, member A (FAM129A), transcript variant 2, mRNA [NM_052966]	1.59
CCL20	Homo sapiens chemokine (C-C motif) ligand 20 (CCL20), transcript variant 1, mRNA [NM_004591]	1.59
GEM	Homo sapiens GTP binding protein overexpressed in skeletal muscle (GEM), transcript variant 1, mRNA [NM_005261]	1.58
PAIP2B	Homo sapiens poly(A) binding protein interacting protein 2B (PAIP2B), mRNA [NM_020459]	1.58
G0S2	Homo sapiens G0/G1 switch 2 (G0S2), mRNA [NM_015714]	1.57
HDAC9	Homo sapiens histone deacetylase 9 (HDAC9), transcript variant 3, mRNA [NM_014707]	1.56
IGF2	Homo sapiens insulin-like growth factor 2 (somatomedin A) (IGF2), transcript variant 1, mRNA [NM_000612]	1.55

Gene symbol	Description	Fold-change
CLDN12	Homo sapiens claudin 12 (CLDN12), mRNA [NM_012129]	1.52
CEP110	Homo sapiens centrosomal protein 110kDa (CEP110), mRNA [NM_007018]	1.50
FLJ35024	Homo sapiens hypothetical LOC401491 (FLJ35024), non-coding RNA [NR_015375]	1.49
MCL1	Homo sapiens myeloid cell leukemia sequence 1 (BCL2-related) (MCL1), transcript variant 1, mRNA [NM_021960]	1.46
HMOX1	Homo sapiens heme oxygenase (decycling) 1 (HMOX1), mRNA [NM_002133]	1.46
KLRC4	Homo sapiens killer cell lectin-like receptor subfamily C, member 4 (KLRC4), mRNA [NM_013431]	1.45
TMEM139	Homo sapiens transmembrane protein 139 (TMEM139), mRNA [NM_153345]	1.45
H19	Homo sapiens H19, imprinted maternally expressed transcript (non-protein coding) (H19), non-coding RNA [NR_002196]	1.45
ZNF165	Homo sapiens zinc finger protein 165 (ZNF165), mRNA [NM_003442]	1.43
HSPA1A	Homo sapiens heat shock 70kDa protein 1A (HSPA1A), mRNA [NM_005345]	1.43
MAFB	Homo sapiens v-maf musculoaponeurotic fibrosarcoma oncogene homolog B (avian) (MAFB), mRNA [NM_005461]	1.42
PNPLA8	Homo sapiens patatin-like phospholipase domain containing 8 (PNPLA8), mRNA [NM_015723]	1.41
C5orf41	Homo sapiens chromosome 5 open reading frame 41 (C5orf41), mRNA [NM_153607]	1.41
LOC643201	Homo sapiens cDNA clone IMAGE:5268504. [BC052945]	1.40
ARMETL1	Homo sapiens arginine-rich, mutated in early stage tumors-like 1 (ARMETL1), mRNA [NM_001029954]	1.40
WDR69	Homo sapiens WD repeat domain 69 (WDR69), mRNA [NM_178821]	1.37
DDIT3	Homo sapiens DNA-damage-inducible transcript 3 (DDIT3), mRNA [NM_004083]	1.35
FOS	Homo sapiens v-fos FBJ murine osteosarcoma viral oncogene homolog (FOS), mRNA [NM_005252]	1.32
ARL5B	Homo sapiens ADP-ribosylation factor-like 5B (ARL5B), mRNA [NM_178815]	1.32
JUN	Homo sapiens jun oncogene (JUN), mRNA [NM_002228]	1.32
ERRFI1	Homo sapiens ERBB receptor feedback inhibitor 1 (ERRFI1), mRNA [NM_018948]	1.31
CCT6B	Homo sapiens chaperonin containing TCP1, subunit 6B (zeta 2) (CCT6B), mRNA [NM_006584]	1.31
TPPP3	Homo sapiens tubulin polymerization-promoting protein family member 3 (TPPP3), mRNA [NM_016140]	1.30

Gene symbol	Description	Fold-change
PPP2R5C	Homo sapiens mRNA; cDNA DKFZp761H0317 (from clone DKFZp761H0317). [AL834350]	1.30
HRK	Homo sapiens harakiri, BCL2 interacting protein (contains only BH3 domain) (HRK), mRNA [NM_003806]	1.27
MALAT1	Homo sapiens metastasis associated lung adenocarcinoma transcript 1 (non-protein coding) (MALAT1), non-coding RNA [NR_002819]	1.27
C4orf16	Homo sapiens chromosome 4 open reading frame 16 (C4orf16), transcript variant 1, mRNA [NM_018569]	1.27
FES	Homo sapiens feline sarcoma oncogene (FES), transcript variant 1, mRNA [NM_002005]	1.27
SDR42E1	Homo sapiens short chain dehydrogenase/reductase family 42E, member 1 (SDR42E1), mRNA [NM_145168]	1.26
LY6K	Homo sapiens lymphocyte antigen 6 complex, locus K (LY6K), mRNA [NM_017527]	1.26
KLHL24	Homo sapiens kelch-like 24 (Drosophila) (KLHL24), mRNA [NM_017644]	1.26
TMEM50B	Homo sapiens transmembrane protein 50B (TMEM50B), mRNA [NM_006134]	1.25
EREG	Homo sapiens epiregulin (EREG), mRNA [NM_001432]	1.25
HK2	Homo sapiens hexokinase 2 (HK2), mRNA [NM_000189]	1.24
RBAK	Homo sapiens RB-associated KRAB zinc finger (RBAK), mRNA [NM_021163]	1.23
RNF6	Homo sapiens ring finger protein (C3H2C3 type) 6 (RNF6), transcript variant 1, mRNA [NM_005977]	1.23
CCL26	Homo sapiens chemokine (C-C motif) ligand 26 (CCL26), mRNA [NM_006072]	1.21
TP53INP1	Homo sapiens tumor protein p53 inducible nuclear protein 1 (TP53INP1), transcript variant 1, mRNA [NM_033285]	1.21
STXBP6	Homo sapiens syntaxin binding protein 6 (amisyn) (STXBP6), mRNA [NM_014178]	1.21
GCAT	Homo sapiens glycine C-acetyltransferase (2-amino-3-ketobutyrate coenzyme A ligase) (GCAT), nuclear gene encoding mitochondrial protein, mRNA [NM_014291]	1.21
SLC2A3P1	Human glucose transporter pseudogene [M55536]	1.21
ZNF765	Homo sapiens zinc finger protein 765 (ZNF765), mRNA [NM_001040185]	1.20
CHST2	Homo sapiens carbohydrate (N-acetylglucosamine-6-O) sulfotransferase 2 (CHST2), mRNA [NM_004267]	1.20
SH3YL1	Homo sapiens SH3 domain containing, Ysc84-like 1 (S cerevisiae) (SH3YL1), mRNA [NM_015677]	1.20

Gene symbol	Description	Fold-change
STX16	Homo sapiens syntaxin 16 (STX16), transcript variant 1, mRNA [NM_001001433]	1.20
ZNF425	Homo sapiens zinc finger protein 425 (ZNF425), mRNA [NM_001001661]	1.19
GPRC5A	Homo sapiens G protein-coupled receptor, family C, group 5, member A (GPRC5A), mRNA [NM_003979]	1.19
MEX3B	Homo sapiens mex-3 homolog B (C. elegans) (MEX3B), mRNA [NM_032246]	1.18
SCML1	Homo sapiens sex comb on midleg-like 1 (Drosophila) (SCML1), transcript variant 1, mRNA [NM_001037540]	1.18
ZNF22	Homo sapiens zinc finger protein 22 (KOX 15) (ZNF22), mRNA [NM_006963]	1.18
ALDOA	Homo sapiens aldolase A, fructose-bisphosphate (ALDOA), transcript variant 2, mRNA [NM_184041]	1.17
SLC22A4	Homo sapiens solute carrier family 22 (organic cation/ergothioneine transporter), member 4 (SLC22A4), mRNA [NM_003059]	1.16
ZNF181	Homo sapiens zinc finger protein 181 (ZNF181), mRNA [NM_001029997]	1.16
LOC728537	Homo sapiens cDNA clone IMAGE:5271446. [BC039374]	1.16
USP36	Homo sapiens cDNA FLJ12851 fis, clone NT2RP2003401, weakly similar to UBIQUITIN CARBOXYL-TERMINAL HYDROLASE DUB-1 (EC 3.1.2.15). [AK022913]	1.15
ZNF600	Homo sapiens zinc finger protein 600 (ZNF600), mRNA [NM_198457]	1.15
SLC6A15	Homo sapiens solute carrier family 6 (neutral amino acid transporter), member 15 (SLC6A15), transcript variant 1, mRNA [NM_182767]	1.15
FBXL19	Homo sapiens F-box and leucine-rich repeat protein 19 (FBXL19), mRNA [NM_001099784]	1.15
CSF2RA	Homo sapiens colony stimulating factor 2 receptor, alpha, low-affinity (granulocyte-macrophage) (CSF2RA), transcript variant 6, mRNA [NM_172249]	1.14
SERP1	Homo sapiens stress-associated endoplasmic reticulum protein 1 (SERP1), mRNA [NM_014445]	1.14
NANOS1	Homo sapiens nanos homolog 1 (Drosophila) (NANOS1), mRNA [NM_199461]	1.13
LOC100131067	Homo sapiens cDNA FLJ38695 fis, clone KIDNE2001897. [AK096014]	1.13
RIMS3	Homo sapiens regulating synaptic membrane exocytosis 3 (RIMS3), mRNA [NM_014747]	1.13
ZNF669	Homo sapiens zinc finger protein 669 (ZNF669), transcript variant 1, mRNA [NM_024804]	1.12